sustainability

MDPI

Article

Method of Predicting Ore Dilution Based on a Neural Network and Its Application

Xingdong Zhao * and Jia'an Niu

Geomechanics Research Center, Northeastern University, Shenyang 110819, China; ja_niu@163.com

* Correspondence: zhaoxingdong@mail.neu.edu.cn; Tel.: +86-135-0490-0292

Received: 27 December 2019; Accepted: 17 February 2020; Published: 19 February 2020

Abstract: A back-propagation neural network prediction model with three layers and six neurons in the hidden layer is established to overcome the limitation of the equivalent linear overbreak slough (ELOS) empirical graph method in estimating unplanned ore dilution. The modified stability number, hydraulic radius, average deviation of the borehole, and powder factor are taken as input variables and the ELOS of quantified unplanned ore dilution as the output variable. The training and testing of the model are performed using 120 sets of data. The average fitting degree r^2 of the prediction model is 0.9761, the average mean square error is 0.0001, and the relative error of the prediction is approximately 6.2%. A method of calculating the unplanned ore dilution is proposed and applied to a test stope of the Sandaoqiao lead–zinc mine. The calculated unplanned ore dilution is 0.717 m, and the relative error (i.e., the difference between calculation and measurement of 0.70 m) is 2.4%, which is better than the relative errors for the empirical graph method and numerical simulation (giving dilution values of 0.8 and 0.55 m, respectively). The back-propagation neural network prediction model is confirmed to predict the unplanned ore dilution in real applications.

Keywords: equivalent linear overbreak slough empirical graph; unplanned ore dilution; back-propagation neural network; prediction model; numerical simulation

---

1. Introduction

Ore dilution control is a common problem in the process of mine production. Unplanned ore dilution refers to the mixing of waste rock into ore not caused by stope design, leading to ore dilution, a higher production cost and a lower quality ore. The accurate and efficient prediction of unplanned ore dilution can guide production by improving the quality of mined ore, mining technology, and production management [1–6].

Scholars have adopted different methods for quantitatively estimating ore dilution. Clark [7] proposed the concept of equivalent linear overbreak slough (ELOS), by which the irregular overcut body under exploitation is transformed into the average overcut depth to represent the unplanned ore dilution value. He introduced the ELOS concept into the stability graph method and proposed the ELOS empirical graph method. Liu et al. [8] obtained a regression equation of the ore recovery rate as a function of the rock inclusion rate of the pillarless sublevel caving on the basis of the simulation results of an ore drawing experiment and the Matlab statistical analysis box. Luo et al. [9] proposed a method of calculating ore dilution using a three-dimensional laser cavity detection system. Tait [10] adopted a neural network to show that the quality of the surrounding rock mass, hydraulic radius of the stope, and various blasting factors are highly correlated with the ELOS. Wang [11] compared measurements of the ELOS with estimations from an empirical graph and concluded that the difference was due to blasting and other factors that have been ignored when building the empirical graph. He also compared the parameters affecting the blasting effect with the previous differences and concluded that the drilling conditions had the main effects on the ELOS. Papaioanou et al. [12] established a stability graph capable of quantifying the ore dilution using two statistical analysis methods, namely the logistic regression and the Bayesian likelihood discrimination. Stewart et al. [13] proposed a method for predicting the dilution of narrow-vein mines on the basis of a large number of examples of narrow-vein mines. Jang et al. [14,15] established a decision support system for unplanned ore dilution using a neuro-fuzzy system. The decision support system provides suggestions for mitigating unplanned ore dilution by analyzing the geology, blasting, and stope design. The above research works are important to the calculation of ore dilution.

In mining production, factors that affect unplanned ore dilution mainly include the stability of surrounding rock, the shape and size of the stope, and the blasting effect of mining. The ELOS empirical graph method proposed by Clark [7] is convenient for the calculation of the unplanned ore dilution of ore but has some disadvantages: (1) When creating the ELOS empirical graph, only the modified stability number and hydraulic radius of the stope are considered, while other factors affecting unplanned ore dilution are ignored, introducing errors into the calculation results; (2) The use of the method is greatly limited once the modified stability number or hydraulic radius exceeds the scale range of the graph; (3) In most cases, the application of the experience graph only provides a fuzzy range of the ELOS and not the exact value. These disadvantages necessitate a more reliable model for predicting unplanned ore dilution in terms of diverse factors.

In this regard, adopting the ELOS empirical graph and fully considering the average deviations of the borehole, powder factor, and other factors affecting the blasting effect, the present paper uses a back-propagation (BP) neural network algorithm to build a model for predicting unplanned ore dilution. The prediction performance of the BP neural network model is modified and optimized using collected data and measurements, and the prediction accuracy of the model is verified by engineering application. The prediction model provides a new method for ore non-dilution index analysis.

2. Materials and Methodologies

2.1. Parameter Selection and Data Acquisition

The present paper determines the modified stability number, hydraulic radius, average deviation of the borehole, powder factor, and the corresponding ELOS as indicators for the analysis and calculation of unplanned ore dilution by comprehensively analyzing the influencing factors, characteristics, and causes of unplanned ore dilution and combining the research results of Clark, Tait, and Wang et al. The established prediction system is shown in Figure 1.

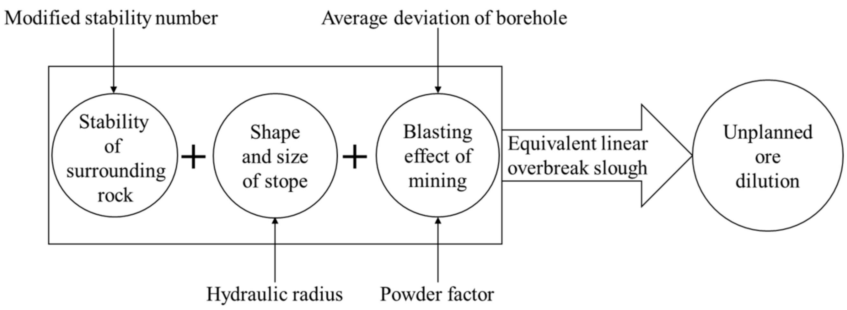

Figure 1. System for predicting unplanned ore dilution.

One hundred sets of basic data of stope unplanned ore dilution at typical mines were collected [11,16–18]. Additionally, rock mechanics tests and three-dimensional laser digital surveying [19] were carried out to obtain 20 sets of data (Table 1). The volume of the overbreak slough of the final stope is obtained by comparing the final stope shape obtained by three-dimensional laser digital surveying with the originally designed stope shape (Figure 2), and the ELOS is calculated as

$$\mathrm{ELOS} = \frac{V_{OS}}{A_S} \tag{1}$$

where V_{OS} is the volume of the slough from the stope surface while A_S is the area of the stope surface.

Table 1. Data for the obtained sample.

Sample Number	Mine	Stope	Modified Stability Number	Hydraulic Radius (m)	Average Borehole Deviation (m)	Powder Factor (kg/t)	ELOS (m)
1	Sandaoqiao	26015	73.10	10.46	0.50	0.50	0.10
2	Sandaoqiao	35052	29.36	12.95	0.60	0.50	1.10
3	Sanshandao	S19170	0.17	1.82	0.20	0.39	2.70
4	Hulun Buir Shanjin	760-7	11.25	7.38	0.40	0.58	1.20
5	Hongling	4102	35.07	8.46	0.40	0.58	0.90
6	Hongling	6113	9.28	6.00	0.30	0.50	0.60
7	Hongling	4100	18.19	13.68	0.60	0.50	1.90
8	Hongtoushan	33	10.39	6.89	0.30	0.45	0.70
9	Hongtoushan	30	6.93	6.89	0.30	0.45	1.10
10	Qinglonggou	3480-4	35.28	4.05	0.40	0.58	0.10
11	Qinglonggou	3480-4	9.18	4.05	0.40	0.58	0.40
12	Qinglonggou	3480-3	35.28	6.12	0.40	0.58	0.10
13	Qinglonggou	3480-3	9.18	6.12	0.40	0.58	0.70
14	Qinglonggou	3500-3	14.03	3.78	0.40	0.39	0.30
15	Qinglonggou	3500-3	3.81	3.78	0.40	0.39	0.80
16	Qinglonggou	3500-2	14.03	5.51	0.40	0.39	0.40
17	Qinglonggou	3500-2	3.81	5.51	0.40	0.39	1.30
18	Qinglonggou	3500-1	14.03	6.51	0.40	0.39	0.40
19	Qinglonggou	3500-1	3.81	6.51	0.40	0.39	1.80
20	Xincheng	632	1.81	1.78	0.20	0.45	1.00

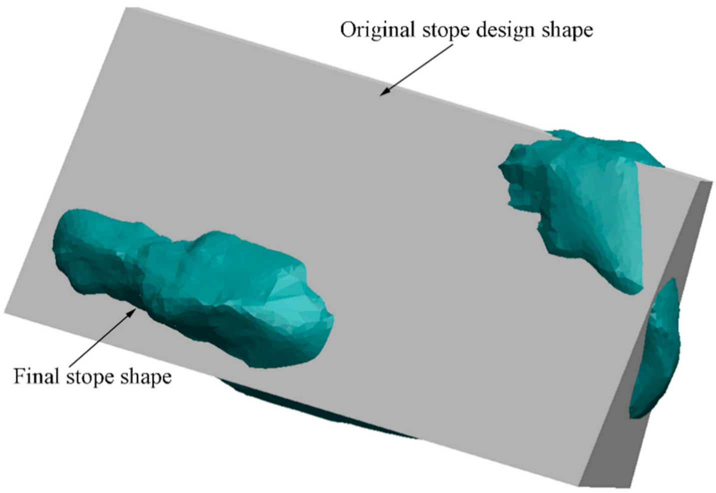

Figure 2. Comparison of the final stope shape and designed stope shape.

The collected data (100 sets) and acquired data (20 sets) constitute the database of the BP neural network model. Eighty percent of the 120 sets of data (i.e., 96 sets of data) are randomly selected as sample data for training the model while the remaining 20% (i.e., 24 sets of data) are selected as the sample data for testing the model.

2.2. Neural Network Model

The unplanned ore dilution is closely related to the modified stability number, hydraulic radius, average deviation of the borehole, and powder factor. However, this complicated relationship is not linear, and it is thus difficult to predict the unplanned ore dilution and the error is relatively large. The BP neural network performs well in handling nonlinear relationships in data. Therefore, the present paper adopts the BP neural network in predicting unplanned ore dilution, effectively reducing the prediction error.

2.2.1. Model Structure

The BP neural network adopted in this paper is a multilayer feedforward neural network based on the error BP algorithm [20–22]. The three-layer BP neural network has excellent nonlinear mapping capability and is thus adopted for modeling in this work [23]; that is, there is one input layer, one hidden layer, and one output layer. The input layer has four input variables, namely the modified stability number, hydraulic radius, average deviation of the borehole, and powder factor, which affect the unplanned ore dilution, and there are thus four neuron nodes in the input layer. The output layer only contains the ELOS, which represents the unplanned ore dilution, and there is thus one neuron node in the output layer. Given that the number of neuron nodes in the hidden layer directly affects the ability of the neural network to map complex problems, the number of neuron nodes in the hidden layer needs to be optimized through experimental analysis; the number is set as n [24].

2.2.2. Building the Model

Due to the five variables—modified stability number, hydraulic radius, drilling of average deviation, powder factor, and ELOS—not being of the same type, they must be normalized to ensure proper training results of the model. The input and output variables are mapped to [0,1] through a normalization processing. The normalization is expressed as

$$z_i{}^k = \frac{Z_i{}^k - Z_{i\min}}{Z_{i\max} - Z_{i\min}}, (k = 1, 2 \cdots 120)(i = 1, 2, 3, 4, 5) \tag{2}$$

where $z_i{}^k$ denotes the normalized data of class I; $Z_i{}^k$ denotes the original data of class i; and $Z_{\min}$ and $Z_{\max}$ are respectively the minimum and maximum values in the original data of class I. After normalization, the input of the model $X_i{}^{(120)} = (x_i{}^1, x_i{}^2 \ldots x_i{}^{120})$ while the expected output $M^{(120)} = (m^1, m^2 \ldots m^{120})$. The input $X_i{}^{(96)}$ of 96 sets of random training samples after normalization processing is input into the neural network, and the output value set $Y_j{}^{(96)}$ of the hidden layer is calculated as

$$Y_j{}^{(96)} = f\left(\sum_{i=1}^{4} w_{ij}{}^{(y)} X_i{}^{(96)} + b_j{}^{(y)}\right) = \frac{1}{1 + e^{-\sum\limits_{i=1}^{4} w_{ij}{}^{(y)} X_i - b_j{}^{(y)}}}, (j = 1, 2 \cdots, n) \tag{3}$$

where $w_{ij}{}^{(y)}$ is the weight of the connection between the input layer and hidden layer; $b_j{}^{(y)}$ is the threshold between the input layer and hidden layer; and the excitation function $f(x)$ of the hidden layer adopts the *logsig* function $f(x) = 1/[1 + \exp(-x)]$. The excitation function of the output layer is set as a linear function. When the input variable propagates forward to the output layer, the set $Z^{(96)}$ of the output of the output layer is calculated as

$$Z^{(96)} = \sum_{j=1}^{n} w_j{}^{(z)} Y_j{}^{(96)} + b^{(z)} \tag{4}$$

where $w_j{}^{(z)}$ is the weight of connection between the hidden layer and output layer while $b^{(z)}$ is the threshold between the hidden layer and output layer. When the output of the output layer of all training samples is obtained, the training accuracy of the model is determined by the mean square error (MSE), expressed as

$$MSE = \frac{1}{96} \sum_{k=1}^{96} \left(m^k - z^k\right)^2 \tag{5}$$

where m^k is the measured ELOS value of the training sample in set k while z^k is the output value of the BP neural network output layer of the training samples in set k. When the error that is the difference between the training output and the measurement is large and the target accuracy is not achieved, the error is reverse-propagated by the gradient descent algorithm until the target accuracy is achieved, which means the training process is complete. The calculation is

$$w_{(N+1)} = w_{(N)} - \alpha \frac{\partial MSE}{\partial w} \tag{6}$$

$$b_{(N+1)} = b_{(N)} - \alpha \frac{\partial MSE}{\partial b} \tag{7}$$

where $w_{(N)}$ is the weight of each connection layer; $b_{(N)}$ is the threshold between the connection layers; $w_{(N+1)}$ is the modified weight; $b_{(N+1)}$ is the revised threshold; α is the network learning rate; and N is the number of corrections.

After the training process, the weights of connection and thresholds between the connecting layers are kept unchanged. The input variable $X_i^{(24)}$ of the remaining 24 test samples after normalization is input into the neural network, and the set of output values $Z^{(24)}$ of the output layer is obtained through the above process. Finally, the output of the output layer in the set is anti-normalized to obtain the predicted value of the test sample.

$$Z_i^k = z_i^k(Z_{i\max} - Z_{i\min}) + Z_{i\min} \tag{8}$$

2.2.3. Model Training and Testing

To ensure the effectiveness of training and testing with sample data, the target error is set as 10^{-4}, the network learning rate is 0.01, and the maximum number of training steps is 1000. A flowchart of the model training and testing is shown in Figure 3.

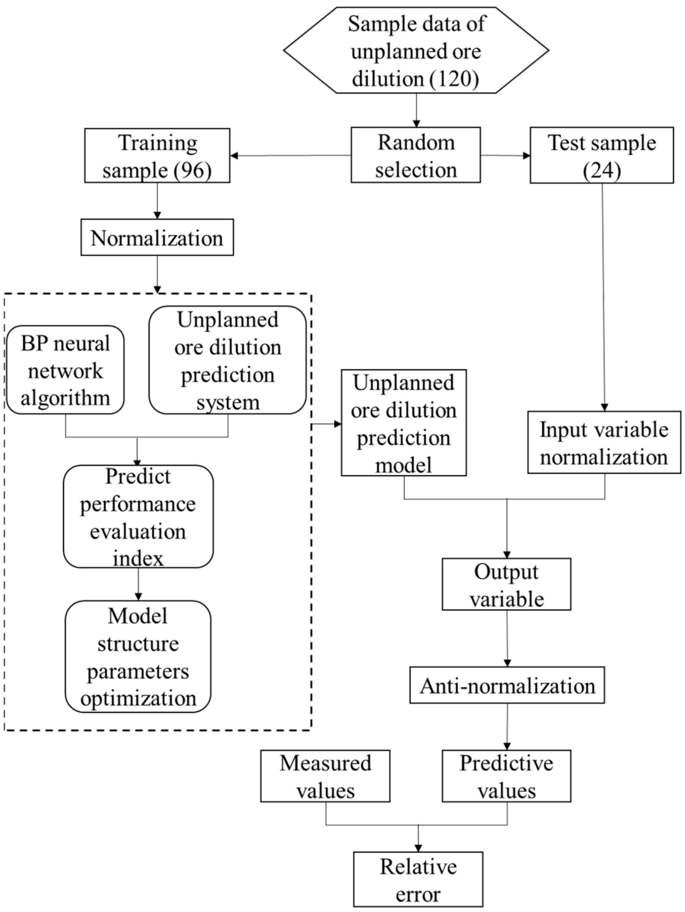

Figure 3. Flowchart of the model training and testing.

The MSE and r^2 are introduced to evaluate the prediction performance of the BP neural network model more comprehensively. As r^2 approaches 1, the correlation between the predicted value and the measurement increases and the fitting degree of the model improves. r^2 is calculated as

$$r^2 = \frac{\left(24\sum_{k=1}^{24} M^k Z^k - \sum_{k=1}^{24} M^k \sum_{k=1}^{24} Z^k\right)^2}{\left[24\sum_{k=1}^{24} (M^k)^2 - \left(\sum_{k=1}^{24} M^k\right)^2\right]\left[24\sum_{k=1}^{24} (Z^k)^2 - \left(\sum_{k=1}^{24} Z^k\right)^2\right]} \tag{9}$$

where M^k is the measured ELOS value of the test sample in set k while Z^k is the predicted ELOS value of the test sample in set k. The number of neuron nodes n in the hidden layer is set as 1–10, and the neural network was trained and tested for 5 times successively to obtain the corresponding predictive performance evaluation index [25] (Table 2).

Table 2. Evaluation index of the prediction performance.

n	Evaluation Index	1st	2nd	3rd	4th	5th	Average Value
1	r^2	0.9372	0.9091	0.8730	0.7650	0.8620	0.8693
	MSE	0.0015	0.0025	0.0038	0.0026	0.0030	0.0027
2	r^2	0.9307	0.8685	0.9390	0.9093	0.8407	0.8976
	MSE	0.0007	0.0007	0.0006	0.0003	0.0010	0.0007
3	r^2	0.9586	0.9124	0.9562	0.8276	0.9351	0.9180
	MSE	0.0004	0.0002	0.0002	0.0002	0.0002	0.0003
4	r^2	0.9633	0.9234	0.8944	0.8847	0.9784	0.9288
	MSE	0.0002	0.0002	0.0002	0.0002	0.0002	0.0002
5	r^2	0.9772	0.9689	0.9117	0.8982	0.9662	0.9444
	MSE	0.0003	0.0002	0.0002	0.0003	0.0007	0.0003
6	r^2	0.9874	0.9700	0.9809	0.9511	0.9909	0.9761
	MSE	0.0001	0.0001	0.0001	0.0001	0.0001	0.0001
7	r^2	0.9810	0.8904	0.9737	0.8993	0.9482	0.9385
	MSE	0.0001	0.0001	0.0001	0.0001	0.0001	0.0001
8	r^2	0.9500	0.9385	0.9633	0.9824	0.9658	0.9600
	MSE	0.0001	0.0001	0.0001	0.0001	0.0002	0.0001
9	r^2	0.9223	0.9390	0.9308	0.9659	0.9376	0.9391
	MSE	0.0001	0.0001	0.0001	0.0001	0.0001	0.0001
10	r^2	0.9325	0.9692	0.9329	0.9171	0.9163	0.9336
	MSE	0.0001	0.0001	0.0001	0.0001	0.0001	0.0001

According to the analysis in Table 2, when there are six neuron nodes in the hidden layer, the average fitting degree r^2 of the BP neural network model is 0.9761 and the average MSE is 0.0001. The prediction performance of the BP neural network model is best in this case. The number of neuron nodes in the hidden layer of the BP neural network model is therefore set at six. Accordingly, the prediction model of unplanned ore dilution is built as the following (Figure 4).

A 5-fold cross-validation experiment was conducted for the established prediction model of unplanned ore dilution. The specific operation process of the experiment was as follows: Step 1: randomly shuffles the database (Appendix A) and divide it into five sets. Step 2: one set is used for test validation set and the other four sets are used for training set. Step 3: after conducting 5 validation tests in turn, randomly shuffles the database again and repeat the first step. The whole process was repeated for 5 times, with a total of 25 experiments for the performance evaluation. The experimental data obtained by 5-fold cross-validation are shown in Appendix B.

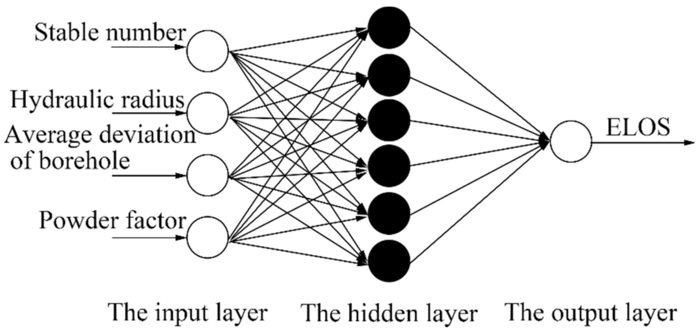

Figure 4. Prediction model of unplanned ore dilution.

Taking the first experimental data of the 5-fold cross-validation experiment as an example, the predicted value of the test samples calculated by the BP neural network model was compared with the measured value, and the results were recorded in Table 3.

Table 3. Comparison of predictions and measurements.

Sample Number	Measured Value (m)	Predicted Value (m)	Relative Error (%)	Sample Number	Measured Value (m)	Predicted Value (m)	Relative Error (%)
1	0.40	0.4016	0.4	13	1.90	1.8510	2.6
2	0.10	0.1096	9.6	14	0.80	0.8726	9.1
3	0.20	0.2179	8.9	15	0.20	0.1932	3.4
4	0.70	0.7025	0.4	16	0.50	0.5363	7.3
5	0.70	0.7625	8.9	17	4.30	4.6840	8.9
6	0.30	0.3256	8.5	18	3.30	3.5360	7.2
7	0.10	0.0984	1.6	19	0.10	0.0896	10.4
8	0.40	0.4363	9.1	20	2.00	2.1350	6.8
9	0.30	0.3260	8.7	21	0.40	0.4254	6.4
10	0.50	0.5104	2.1	22	0.80	0.7242	9.5
11	0.60	0.5619	6.4	23	0.90	0.9262	2.9
12	0.90	0.8672	3.6	24	1.10	1.1210	1.9

The corresponding data in Table 3 are integrated to draw a relative error diagram of the unplanned ore dilution prediction model, as shown in Figure 5.

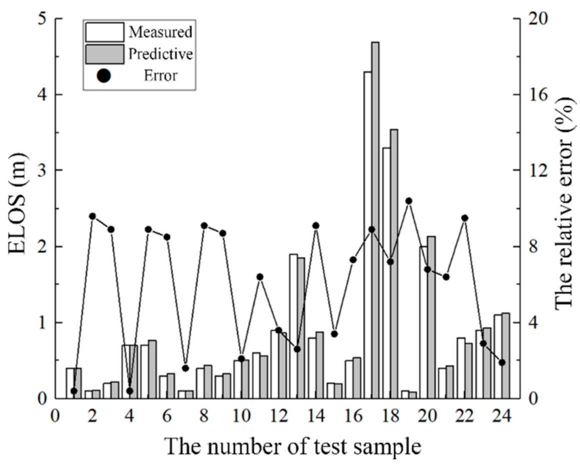

Figure 5. Prediction error.

The Figure 5 reveals that the predicted value is slightly different from the field measurements, with the average relative error being 6.0%. The relative error of each test sample fluctuates within a certain range, and the fluctuation range is insignificant (10%). Using the same method to deal with the other data obtained from the 5-fold cross-validation experiments, the relative error between the predicted value of the unplanned ore dilution prediction model and the measured value in the field is within 19.6%. The mean relative error was 6.2%. Therefore, the prediction model of unplanned ore dilution based on the BP neural network has good accuracy and stability.

2.2.4. Calculation of Unplanned Ore Dilution

Table 2 shows that the prediction performance for unplanned ore dilution is best when there are six neuron nodes in the hidden layer. However, when deriving the formula for calculating the unplanned ore dilution, the increase in the number of neuron nodes in the hidden layer greatly increases the complexity of formula derivation. Therefore, the hidden layer neuron node is reduced to one, while other layer neuron node remains unchanged, and the formula is derived.

The input variables are normalized to X_1, X_2, X_3, and X_4 using Formula (2) and the output y of the hidden layer is obtained by substituting the input variables X_1, X_2, X_3, and X_4 into Formula (3):

$$y = 1/1 + \exp(-{w_1}^{(y)}X_1 - {w_2}^{(y)}X_2 - {w_3}^{(y)}X_3 - {w_4}^{(y)}X_4 - b^{(y)}) \tag{10}$$

The output y of the hidden layer is input into Formula (4) to get the output z of the output layer:

$$z = b^{(z)} + w^{(z)}/1 + \exp(-{w_1}^{(y)}X_1 - {w_2}^{(y)}X_2 - {w_3}^{(y)}X_3 - {w_4}^{(y)}X_4 - b^{(y)}) \tag{11}$$

where the weight of the input layer to the hidden layer ${w_i}^{(y)}$ = {2.5610, −1.5110, 0.0536, −0.0845}; the threshold $b^{(y)}$ = 2.2195; the weight of the connection from the hidden layer to the output layer ${w_i}^{(z)}$ = −1.4773; and the threshold $b^{(z)}$ = 0.4850.

The input and output values in Formula (11) are anti-normalized to obtain the formula for calculating the unplanned ore dilution (i.e., ELOS).

$$\text{ELOS} = 0.4850 - 6.3524/1 + \exp(-0.0362x_1 + 0.0819x_2 - 0.0447x_3 + 0.0871x_4 - 2.3240) \tag{12}$$

2.3. *Empirical Graph Method*

ELOS empirical graph method [7] is the common method used to estimate the unplanned ore dilution. Although empirical graph method has some shortcomings, it can also verify the prediction performance of neural network. The empirical graph for estimating unplanned ore dilution is shown in Figure 6.

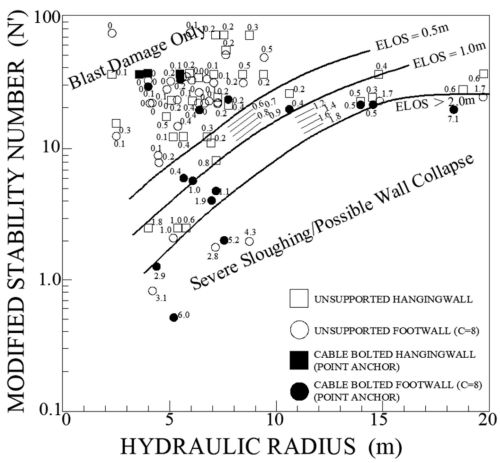

Figure 6. ELOS empirical graph.

2.4. Numerical Simulation Method

With the continuous development and improvement of computer levels, numerical calculation software has been widely used in geotechnical engineering analysis. As a common verification method, numerical simulation has the advantages of providing intuitive results and having strong applicability.

In this paper, RS2 numerical simulation software was used to verify the predictive performance of the established neural network model. RS2 is a powerful geotechnical finite element analysis software developed by Rocscience, which can perform a certain degree of predictive analysis before engineering construction.

3. Results

3.1. Engineering Application

In order to verify and cross-validate the BP neural network approach, we select a test stope in the Sandaoqiao lead-zinc mine to analyze and calculate the unplanned ore dilution and verify the accuracy of the calculation.

3.1.1. Geological Setting and Engineering Background

The Sandaoqiao lead-zinc mine is located on the western margin of the northern section of the Greater Khingan Range in Inner Mongolia, China (Figure 7). There are 67 lead-zinc industrial orebodies in the ore belts I, II, and III within the mining area, among which orebody III-3 is the largest. This orebody has a strike of 286°–345° and dip angle of 70°–85°. The orebody is vein-shaped and regular in shape. The middle part of the ore body is thicker than the deep part and both sides.

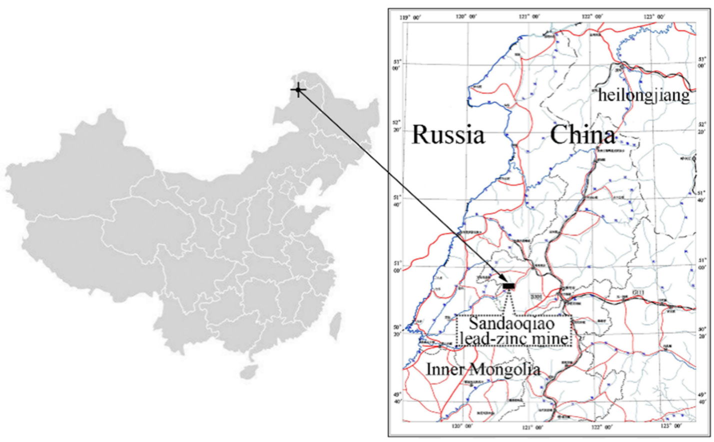

Figure 7. Location of the Sandaoqiao lead–zinc mine.

The stope of the Sandaoqiao lead-zinc mine had a length of 50 m and a height of 40 m. When mining in an area neighboring exploration line 9 at a depth of 610 m for orebody III-3, the occurrence of geological faults resulted in the serious dislocation of orebody III-3 and a length of the remaining orebody of 80 m. If two stopes are arranged for the length of an orebody, the amount of mining and cutting works and the cost of mining are greatly increased. In an effort to reduce costs and improve production, the mine lengthened the stope from 50 to 80 m. Consequently, only one stope is needed to extract the remaining ore of orebody III-3 at a depth of 610 m, which greatly reduces the cutting quantity and recovery cost. However, the problem is that a change in stope size will affect unplanned ore dilution, and previous experience of unplanned ore dilution of the original stope size is no longer valid in predicting unplanned ore dilution with a larger stope. It is therefore necessary to use the prediction model to obtain the unplanned ore dilution for a test stope.

3.1.2. Test Stope

The selected test stope of orebody III-3 at a depth of 610 m at the Sandaoqiao lead-zinc mine is between exploration lines 5 and 9 (Figure 8).

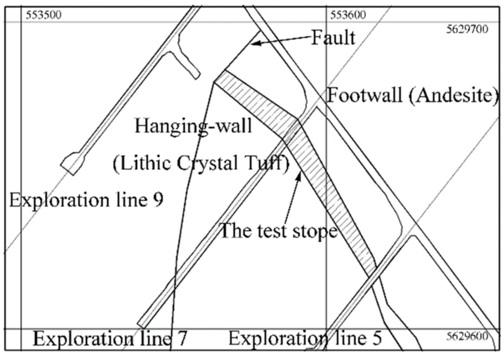

Figure 8. Position of the test stope.

The test stope has an average span of 5 m, a height of 40 m, a strike length of 80 m, and an inclination angle of 70°. The surrounding rock of the hanging wall of the test stope is detritus crystal tuff while the surrounding rock of the footwall is andesite. The mining method is shallow-hole shrinkage mining with a flat bottom structure (Figure 9).

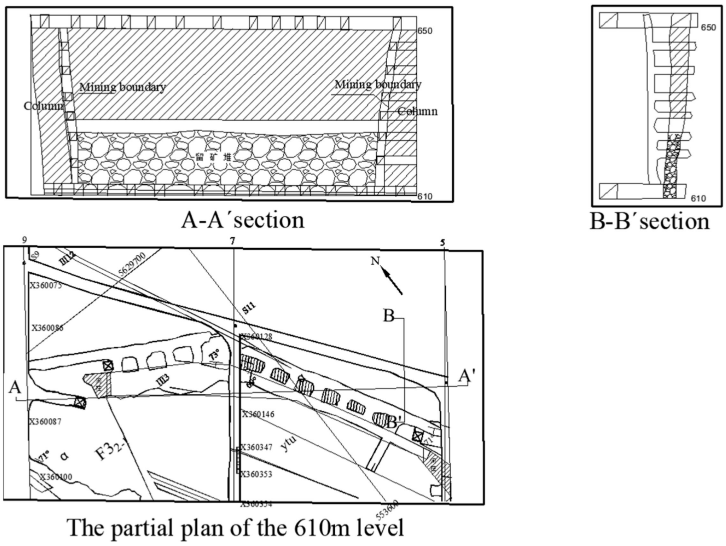

Figure 9. Method of mining the test stope.

3.1.3. Model Application

Various parameters affecting stope stability are obtained from an engineering geological survey and rock mechanics tests of the test stope (Table 4).

Table 4. Parameters of the hanging wall ELOS.

Modified Stability Number	Hydraulic Radius (m)	Average Borehole Deviation (m)	Powder Factor (kg/t)
41.06	13.89	0.60	0.50

Parameters in Table 4 are taken as input variables for the unplanned-dilution prediction model based on a BP neural network. At the end of model training, the MSE is 9×10^{-5}, and the calculated ELOS of the hanging wall of the test stope is 0.717 m.

3.2. Comparison and Analysis

Results obtained using the BP neural network model are verified by comparing the field measurements of the ELOS with results obtained using the BP neural network prediction method, the empirical graph method, and the numerical simulation method.

3.2.1. Results of Empirical Graph Method

The ELOS empirical graph is the common approach of estimating unplanned ore dilution. The modified stability number and hydraulic radius in Table 4 are added to the ELOS empirical graph, and the position of the test stope at a depth of 610 m for the Sandaoqiao lead-zinc mine is obtained as shown in Figure 10.

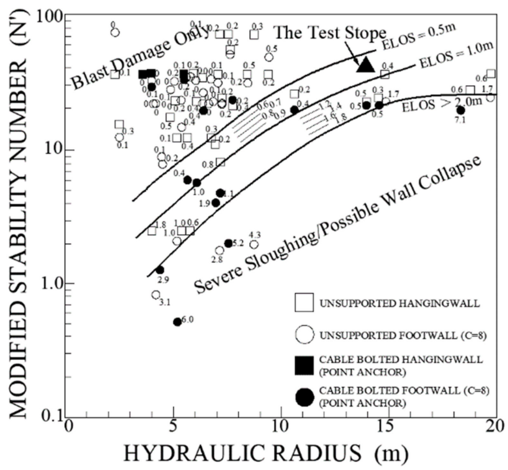

Figure 10. ELOS empirical graph.

Figure 10 shows that the ELOS of the test stope obtained using the ELOS empirical graph method is approximately 0.8 m.

3.2.2. Results of Numerical Simulation

In this paper, RS2 software is used to analyze the mining of the test stope of the Sandaoqiao lead-zinc mine. The specific process of simulation is not explained here [26]. Numerical results are presented in Figure 11.

Figure 11. Contours of the plastic zone.

The morphology of the plastic zone shown in Figure 11 reveals that the ELOS of the hanging wall of the test stope is 0.55 m.

Field measurements (Figure 12), results obtained using the BP neural network prediction method and empirical graph method, and numerical simulation results are compared in Table 5. The results show that the BP neural network prediction model performs well.

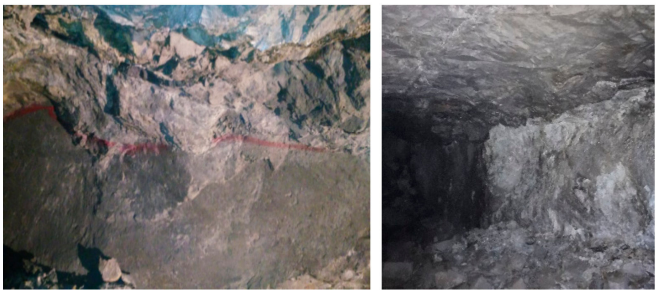

(**a**) Hanging wall

(**b**) Crown

(**c**) Footwall

Figure 12. Field photographs of the test stope.

Table 5. Comparison of results of investigative methods.

Research Methods	ELOS (m)	Relative Error (%)
Field measured	0.70	0
BP neural network prediction method	0.717	2.4
Empirical graph method [7]	0.8	14.3
Numerical simulation analysis	0.55	21.4

4. Discussion

In order to more accurately and effectively predict ore dilution, based on the ELOS empirical graph method and fully considering the average deviations of the borehole, powder factor, and other factors affecting the blasting quality, a prediction model of unplanned ore dilution based on a three-layer BP neural network with six neuron nodes in the hidden layer was established. Using collected and measured data to modify and evaluate the predictive performance of the model, the unplanned ore dilution prediction model was used to calculate the test stope of Sandaoqiao lead-zinc mine, and the ELOS of hanging wall was 0.717 m. The relative error between the predicted and actual measurements was 2.4%. Therefore, the established prediction model is accurate and reasonable, which provides a new method for the quantitative analysis of unplanned ore dilution.

Although the traditional ELOS empirical graph method is convenient to use, it has the disadvantages of not being able to give precise values and being limited in application range. The BP neural network model established in this paper performs well in predicting the unplanned ore dilution. The average relative error of the prediction model is 6.2% after the 5-fold cross-validation experiment. Therefore, the prediction method of ore dilution based on neural network has a wider application range with good accuracy, making up for the shortcomings of ELOS empirical graph.

A limitation of the unplanned ore dilution prediction model is that it is complicated to use. The next research objective is to simplify the operation procedure and improve the accuracy of the simplified calculation formula.

5. Conclusions

Data of unplanned ore dilution for actual mines (i.e., the modified stability number, hydraulic radius, average borehole deviation, and powder factor) were collected and a model of unplanned ore dilution was established on the basis of a BP neural network. The average fitting degree r^2 of the model was 0.9761, the average MSE was 0.0001, and the relative error of prediction was about 6.2%. By referring to the BP neural network model, the simplified calculation formula of unplanned ore dilution based on a single hidden layer neuron is derived, which provides another research method for quantitative ore dilution.

Calculations were made for a test stope of the Sandaoqiao lead-zinc mine by applying the unplanned ore dilution prediction model, and the ELOS of the hanging wall of 0.717 m was obtained. The difference between calculation and measurement was 2.4%, which is better than the relative error when adopting the graph method (relative error of 14.3%) or that when conducting numerical simulation (relative error of 21.4%). The results show that the BP neural network model can be effectively applied in predicting unplanned ore dilution, providing a new method for ore dilution analysis.

Author Contributions: X.Z. conceived and designed the research. J.N. performed the field investigations and experiments, collected the field data. J.N. wrote the original manuscript. X.Z. revised the manuscript. All authors have read and agreed to the published version of the manuscript.

Funding: This research was funded by the National Key Research and Development Program (2018YFC0604604, 2018YFC0604401, and 2016YFC0600803) and Project of the NSFC-Shandong United Fund (U1806208).

Conflicts of Interest: The authors declare no conflict of interest.

Appendix A

Table A1. Database of 120 case histories of unplanned ore dilution.

Sample Number	Modified Stability Number	Hydraulic Radius (m)	Average Borehole Deviation (m)	Powder Factor (kg/t)	ELOS (m)
1	73.10	10.46	0.50	0.50	0.10
2	29.36	12.95	0.60	0.50	1.10
3	0.17	1.82	0.20	0.39	2.70
4	11.25	7.38	0.40	0.58	1.20
5	35.07	8.46	0.40	0.58	0.90
6	9.28	6.00	0.30	0.50	0.60
7	18.19	13.68	0.60	0.50	1.90
8	10.39	6.89	0.30	0.45	0.70
9	6.93	6.89	0.30	0.45	1.10
10	35.28	4.05	0.40	0.58	0.10
11	9.18	4.05	0.40	0.58	0.40
12	35.28	6.12	0.40	0.58	0.10

Table A1. *Cont.*

Sample Number	Modified Stability Number	Hydraulic Radius (m)	Average Borehole Deviation (m)	Powder Factor (kg/t)	ELOS (m)
13	9.18	6.12	0.40	0.58	0.70
14	14.03	3.78	0.40	0.39	0.30
15	3.81	3.78	0.40	0.39	0.80
16	14.03	5.51	0.40	0.39	0.40
17	3.81	5.51	0.40	0.39	1.30
18	14.03	6.51	0.40	0.39	0.40
19	3.81	6.51	0.40	0.39	1.80
20	1.81	1.78	0.20	0.45	1.00
21	8.10	7.00	0.50	0.56	0.80
22	11.00	7.40	0.60	0.41	1.30
23	7.00	8.80	0.60	0.64	2.30
24	11.00	7.30	0.70	0.45	2.10
25	7.10	9.30	1.00	0.95	1.30
26	8.80	6.90	0.10	0.59	0.10
27	7.80	7.60	0.60	0.41	1.10
28	8.80	6.70	0.70	0.86	2.10
29	7.30	7.20	0.30	0.36	1.20
30	7.80	6.90	0.70	0.45	1.90
31	10.80	5.00	0.50	0.41	0.60
32	8.00	7.20	0.4	0.40	1.20
33	12.20	6.60	0.20	0.40	0.20
34	11.40	6.70	0.30	0.41	0.50
35	6.70	7.30	0.20	0.59	1.10
36	12.00	6.20	0.20	0.60	0.40
37	9.90	9.10	0.4	0.88	1.40
38	14.10	5.40	0.40	0.37	0.20
39	9.20	6.00	0.60	0.45	0.50
40	12.20	6.60	0	0.43	0.30
41	11.20	5.50	0	0.59	0.40
42	11.10	5.20	0.50	0.52	0.40
43	6.00	5.50	0.75	1.05	3.30
44	11.10	6.20	0	0.40	0.40
45	11.60	6.50	0.50	0.50	0.60
46	6.30	8.00	1.00	0.41	4.40
47	9.80	7.00	1.20	0.28	4.00
48	12.00	6.30	0.40	0.32	0.70
49	13.50	6.90	0.40	0.54	0.60
50	9.80	7.50	0.50	0.32	0.80
51	11.00	6.00	0.40	0.67	0.40
52	10.10	8.10	0.90	0.51	1.10
53	9.50	6.20	0.80	0.47	0.70
54	10.30	6.30	0.70	0.47	0.60
55	8.20	6.00	0.90	0.29	1.10
56	7.70	5.60	0.90	0.47	1.50
57	8.20	5.70	0.90	0.36	2.40
58	9.10	5.70	0.30	0.31	0.80
59	10.40	6.90	0.60	0.57	0.80
60	10.60	5.70	0.70	0.33	0.40
61	4.50	7.20	1.00	0.30	1.90
62	7.90	7.20	0	0.30	0.90
63	3.80	7.00	0.50	0.25	1.90
64	5.40	6.10	0.90	0.25	1.20
65	5.60	5.70	0	0.45	0.40
66	12.00	5.70	0	0.45	0.30
67	1.70	7.20	0	0.60	2.80

Table A1. *Cont.*

Sample Number	Modified Stability Number	Hydraulic Radius (m)	Average Borehole Deviation (m)	Powder Factor (kg/t)	ELOS (m)
68	7.20	7.20	0	0.60	0.20
69	1.90	8.80	0	0.40	4.30
70	72.00	8.80	0	0.40	0.20
71	1.90	7.60	0	0.55	5.20
72	72.00	7.60	0	0.55	0.10
73	34.00	10.20	0	0.40	0
74	18.20	4.50	0	0.39	0.20
75	21.60	4.50	0	0.39	0.10
76	21.60	7.30	0.60	0.31	0.30
77	21.60	7.30	0.60	0.31	0.30
78	21.60	6.70	1.10	0.32	0.50
79	21.60	6.40	0.90	0.32	0.40
80	1.20	4.40	0	0.70	2.90
81	22.50	15.00	0.25	0.65	1.90
82	36.00	15.00	0.25	0.65	1.00
83	22.50	20.00	0.25	0.65	4.10
84	36.00	20.00	0.25	0.65	1.70
85	34.00	5.80	0.60	0.90	0.10
86	2.40	5.80	0.30	0.90	2.00
87	12.00	2.50	0.40	0.50	0.10
88	15.00	2.50	0.40	0.50	0.30
89	23.00	5.40	0.50	1.20	0.20
90	2.40	5.40	0.10	1.20	1.80
91	22.00	4.10	0.10	1.10	0.20
92	23.00	4.10	0.10	1.10	0.10
93	29.00	4.00	0.50	0.58	0.10
94	36.00	4.00	0.95	0.58	0.10
95	32.00	4.00	0.30	0.90	0.10
96	2.40	4.00	0.15	0.90	1.10
97	22.00	4.20	0.10	1.20	0.10
98	23.00	4.20	0.10	1.20	0
99	32.00	5.10	0.30	0.63	0.30
100	23.00	5.10	0.40	0.63	0.20
101	14.50	5.40	0.50	1.00	0.40
102	2.40	5.40	0.15	1.00	1.80
103	35.00	5.60	0	1.14	0.10
104	23.00	5.60	0	1.14	0.30
105	26.00	6.40	0.80	0.65	0.20
106	34.00	6.40	0.50	0.65	0.10
107	28.00	4.90	1.00	0.47	0.40
108	17.00	4.90	0.45	0.47	0.40
109	22.40	6.90	0.40	0.84	0.20
110	23.00	6.90	0.30	0.84	0.20
111	10.50	5.60	0.30	1.19	0.40
112	23.00	5.60	0	1.19	0.20
113	2.00	5.20	0.50	0.64	1.80
114	12.00	5.20	0.50	0.64	0.50
115	31.00	7.10	0.15	0.84	0.20
116	36.00	7.10	0.15	0.84	0.10
117	33.00	5.50	0.15	1.05	0.10
118	7.10	8.10	0	0.35	1.60
119	60.00	7.90	0.50	0.45	0.20
120	7.20	7.30	0	1.22	1.20

Appendix B

Table A2. Experimental results of 5-fold cross-validation.

Sample Number	Measured Value (m)	Predicted Value (m)	Relative Error (%)	Sample Number	Measured Value (m)	Predicted Value (m)	Relative Error (%)
			I-1				
1	0.40	0.4016	0.4	13	1.90	1.8510	2.6
2	0.10	0.1096	9.6	14	0.80	0.8726	9.1
3	0.20	0.2179	8.9	15	0.20	0.1932	3.4
4	0.70	0.7025	0.4	16	0.50	0.5363	7.3
5	0.70	0.7625	8.9	17	4.30	4.6840	8.9
6	0.30	0.3256	8.5	18	3.30	3.5360	7.2
7	0.10	0.0984	1.6	19	0.10	0.0896	10.4
8	0.40	0.4363	9.1	20	2.00	2.1350	6.8
9	0.30	0.3260	8.7	21	0.40	0.4254	6.4
10	0.50	0.5104	2.1	22	0.80	0.7242	9.5
11	0.60	0.5619	6.4	23	0.90	0.9262	2.9
12	0.90	0.8672	3.6	24	1.10	1.1210	1.9
			I-2				
1	2.70	2.8167	4.3	13	1.80	1.7164	4.6
2	0.00	0.0125	-	14	1.80	1.8591	3.3
3	1.10	1.1294	2.7	15	0.40	0.3916	2.1
4	0.10	0.1165	16.5	16	0.10	0.0898	10.2
5	0.20	0.2088	4.4	17	0.20	0.2211	10.6
6	0.40	0.4376	9.4	18	0.20	0.2017	0.8
7	0.70	0.6153	12.1	19	1.70	1.5946	6.2
8	1.00	1.0768	7.7	20	1.10	1.0579	3.8
9	1.30	1.3013	0.1	21	1.20	1.1350	5.4
10	0.20	0.1936	3.2	22	0.20	0.1960	2.0
11	0.20	0.1867	6.7	23	0.10	0.0863	13.7
12	0.20	0.1962	1.9	24	1.80	2.0341	13.0
			I-3				
1	0.40	0.4312	7.8	13	0.20	0.1843	7.9
2	0.10	0.1163	16.3	14	1.90	2.1185	11.5
3	0.10	0.0897	10.3	15	2.40	2.5134	4.7
4	0.40	0.3848	3.8	16	4.10	4.2107	2.7
5	0.40	0.4132	3.3	17	0.60	0.5861	2.3
6	0.40	0.4076	1.9	18	0.40	0.4166	4.2
7	0.30	0.3189	6.3	19	2.30	2.5427	10.6
8	1.60	1.6931	5.8	20	0.30	0.3166	5.5
9	0.40	0.3977	0.6	21	0.20	0.1843	7.9
10	1.20	1.2694	5.8	22	0.00	0.0000	-
11	0.30	0.2849	5.0	23	1.20	1.2309	2.6
12	1.90	2.1067	10.9	24	0.10	0.1129	12.9
			I-4				
1	1.30	1.3351	2.7	13	1.40	1.3527	3.4
2	1.20	1.1964	0.3	14	2.80	3.1640	13.0
3	2.90	3.1360	8.1	15	5.20	4.9937	4.0
4	2.10	2.2034	4.9	16	1.80	1.8324	1.8
5	1.10	1.0875	1.1	17	1.10	1.2165	10.6
6	1.50	1.6137	7.6	18	0.10	0.1183	18.3
7	0.60	0.5873	2.1	19	1.30	1.3065	0.5
8	4.00	3.8992	2.5	20	0.40	0.4324	8.1
9	0.80	0.8443	5.5	21	0.80	0.8735	9.2
10	0.40	0.4385	9.6	22	1.90	2.0415	7.4
11	0.40	0.3768	5.8	23	1.10	1.1216	2.0
12	0.10	0.0879	12.1	24	0.60	0.6370	6.2

Table A2. *Cont.*

Sample Number	Measured Value (m)	Predicted Value (m)	Relative Error (%)	Sample Number	Measured Value (m)	Predicted Value (m)	Relative Error (%)
			I-5				
1	0.30	0.2843	5.2	13	0.50	0.4735	5.3
2	1.90	1.8463	2.8	14	0.60	0.5783	3.6
3	0.20	0.2174	8.7	15	0.10	0.1008	0.8
4	0.30	0.3149	5.0	16	0.20	0.2101	5.1
5	0.10	0.0889	11.1	17	0.80	0.8345	4.3
6	0.40	0.3974	0.7	18	2.10	2.0762	1.1
7	0.20	0.1865	6.8	19	0.10	0.1015	1.5
8	0.30	0.3348	11.6	20	0.10	0.0991	0.9
9	0.10	0.1176	17.6	21	1.20	1.2016	0.1
10	1.10	1.2840	16.7	22	0.50	0.4870	2.6
11	4.40	4.0957	6.9	23	1.00	1.1047	10.5
12	0.70	0.6782	3.1	24	0.10	0.0985	1.5
			II-1				
1	1.90	1.8967	0.2	13	0.20	0.1980	1.0
2	0.40	0.3955	1.1	14	1.90	2.0766	9.3
3	0.10	0.1103	10.3	15	0.40	0.3754	6.2
4	0.40	0.4124	3.1	16	0.10	0.0955	4.5
5	0.20	0.2067	3.3	17	0.10	0.0956	4.4
6	2.40	2.4348	1.5	18	0.80	0.7872	1.6
7	1.10	1.0846	1.4	19	0.70	0.7216	3.1
8	4.30	4.2841	0.4	20	0.40	0.3862	3.5
9	0.70	0.8346	19.2	21	0.10	0.1106	10.6
10	0.10	0.0968	3.2	22	0.70	0.7416	5.9
11	1.20	1.2167	1.4	23	1.20	1.4345	19.5
12	0.20	0.2164	8.2	24	1.10	1.2000	9.1
			II-2				
1	1.30	1.3355	2.7	13	0.10	0.1056	5.6
2	1.80	1.7645	2.0	14	1.30	1.3110	0.8
3	0.20	0.2046	2.3	15	0.20	0.2249	12.5
4	1.10	1.1312	2.8	16	1.10	1.1041	0.4
5	0.40	0.3986	0.4	17	0.80	0.7835	2.1
6	1.70	1.6843	0.9	18	0.40	0.4338	8.5
7	1.10	1.0764	2.1	19	0.30	0.3154	5.1
8	0.30	0.2845	5.2	20	0.40	0.4314	7.9
9	0.40	0.4061	1.5	21	0.20	0.2135	6.7
10	0.50	0.5137	2.7	22	0.80	0.8376	4.7
11	0.00	0.0800	-	23	0.20	0.2357	17.9
12	0.20	0.2164	8.2	24	2.00	2.3014	15.1
			II-3				
1	1.00	1.1435	14.4	13	0.10	0.0947	5.3
2	0.60	0.5913	1.4	14	1.30	1.4157	8.9
3	1.90	2.1438	12.8	15	2.30	2.4180	5.1
4	2.70	2.8375	5.1	16	5.20	5.5438	6.6
5	0.50	0.4971	0.6	17	2.80	2.7641	1.3
6	1.10	1.0090	8.3	18	3.30	3.3264	0.8
7	0.60	0.5763	3.9	19	0.30	0.3275	9.2
8	0.60	0.5816	3.1	20	0.20	0.1800	10.0
9	1.20	1.3244	10.4	21	4.40	4.1826	4.9
10	0.00	0.0676	-	22	0.30	0.3156	5.2
11	0.20	0.2276	13.8	23	4.00	4.3468	8.7
12	4.10	3.5762	12.8	24	0.40	0.4380	9.5

Table A2. *Cont.*

Sample Number	Measured Value (m)	Predicted Value (m)	Relative Error (%)	Sample Number	Measured Value (m)	Predicted Value (m)	Relative Error (%)
			II-4				
1	1.50	1.4863	0.9	13	2.10	2.1642	3.1
2	0.20	0.1963	1.9	14	0.20	0.2039	1.9
3	0.40	0.4338	8.5	15	1.90	1.8630	1.9
4	1.10	1.1008	0.1	16	1.80	1.8345	1.9
5	0.10	0.0950	5.0	17	0.90	0.8935	0.7
6	0.40	0.3746	6.4	18	0.10	0.1107	10.7
7	0.80	0.7641	4.5	19	0.20	0.2143	7.1
8	1.80	1.7634	2.0	20	1.20	1.2400	3.3
9	0.50	0.5166	3.3	21	2.10	2.0613	1.8
10	0.40	0.4176	4.4	22	0.10	0.1031	3.1
11	0.60	0.5834	2.8	23	2.90	2.6137	9.9
12	0.70	0.6945	0.8	24	0.30	0.2860	4.7
			II-5				
1	0.50	0.4791	4.2	13	0.10	0.1196	19.6
2	0.10	0.1037	3.7	14	0.10	0.0964	3.6
3	0.10	0.0963	3.7	15	0.30	0.3167	5.6
4	0.20	0.2048	2.4	16	0.80	0.7315	8.6
5	1.80	1.9115	6.2	17	0.10	0.0846	15.4
6	0.40	0.4310	7.7	18	0.90	0.9153	1.7
7	0.40	0.4135	3.4	19	1.60	1.7346	8.4
8	0.10	0.1164	16.4	20	0.30	0.2872	4.3
9	1.00	1.1866	18.7	21	1.20	1.1631	3.1
10	0.60	0.6423	7.1	22	0.40	0.4232	5.8
11	1.90	2.0409	7.4	23	1.40	1.3451	3.9
12	0.10	0.0900	10.0	24	0.30	0.2900	3.3
			III-1				
1	0.10	0.1119	11.9	13	1.80	1.8635	3.5
2	4.40	4.5341	3.0	14	0.10	0.1086	8.6
3	0.10	0.1035	3.5	15	1.30	1.3107	0.8
4	0.30	0.3321	10.7	16	0.80	0.8647	8.1
5	5.20	4.9314	5.2	17	0.80	0.7961	0.5
6	0.20	0.1937	3.2	18	1.20	1.2418	3.5
7	1.10	1.2107	10.1	19	2.00	1.8937	5.3
8	1.80	2.0310	12.8	20	0.10	0.0864	13.6
9	0.40	0.4213	5.3	21	1.20	1.3000	8.3
10	0.40	0.3938	1.6	22	0.60	0.6374	6.2
11	0.40	0.3896	2.6	23	0.10	0.1132	13.2
12	0.10	0.1129	12.9	24	0.30	0.3571	19.0
			III-2				
1	0.60	0.6138	2.3	13	0.40	0.4134	3.3
2	0.90	1.0336	14.8	14	0.20	0.1763	11.9
3	1.30	1.2861	1.1	15	0.30	0.3224	7.5
4	4.10	3.8630	5.8	16	2.40	2.3100	3.7
5	0.40	0.4267	6.7	17	0.10	0.0913	8.7
6	3.30	3.0492	7.6	18	1.30	1.2763	1.8
7	0.30	0.3215	7.2	19	0.70	0.6847	2.2
8	0.50	0.5553	11.1	20	0.20	0.1965	1.8
9	1.80	1.8647	3.6	21	0.30	0.2934	2.2
10	1.50	1.4682	2.1	22	0.90	0.9738	8.2
11	1.70	1.7134	0.8	23	0.40	0.4318	8.0
12	1.90	2.1040	10.7	24	0.30	0.3221	7.4

Table A2. *Cont.*

Sample Number	Measured Value (m)	Predicted Value (m)	Relative Error (%)	Sample Number	Measured Value (m)	Predicted Value (m)	Relative Error (%)
			III-3				
1	0.10	0.1002	0.2	13	0.10	0.1132	13.2
2	0.40	0.4231	5.8	14	1.00	1.1016	10.2
3	2.10	2.1430	2.0	15	1.90	2.1034	10.7
4	0.10	0.0972	2.8	16	0.70	0.6978	0.3
5	1.00	1.0434	4.3	17	1.20	1.0967	8.6
6	0.10	0.1109	10.9	18	0.20	0.1846	7.7
7	0.10	0.0883	11.7	19	0.60	0.6324	5.4
8	0.80	0.7966	0.4	20	2.70	2.9647	9.8
9	0.80	0.7990	0.1	21	1.10	1.2155	10.5
10	0.40	0.4235	5.9	22	0.50	0.4863	2.7
11	1.90	2.0137	6.0	23	0.40	0.4129	3.2
12	0.20	0.2106	5.3	24	0.30	0.3336	11.2
			III-4				
1	0.20	0.2130	6.5	13	0.10	0.0954	4.6
2	1.40	1.3765	1.7	14	0.20	0.1861	7.0
3	0.50	0.5111	2.2	15	0.40	0.4213	5.3
4	0.20	0.2200	10.0	16	0.40	0.4255	6.4
5	1.20	1.2135	1.1	17	0.20	0.2131	6.6
6	0.70	0.6813	2.7	18	0.10	0.0876	12.4
7	0.20	0.2164	8.2	19	0.20	0.2137	6.9
8	0.00	0.0720	-	20	0.20	0.2190	9.5
9	0.40	0.4422	10.6	21	0.00	0.0000	-
10	0.30	0.3231	7.7	22	4.00	4.2347	5.9
11	1.90	2.1348	12.4	23	0.80	0.7889	1.4
12	0.10	0.1090	9.0	24	1.10	1.2011	9.2
			III-5				
1	0.20	0.2115	5.7	13	2.80	2.7648	1.3
2	1.10	1.1341	3.1	14	0.40	0.4344	8.6
3	1.60	1.6340	2.1	15	0.50	0.5346	6.9
4	2.90	3.1021	7.0	16	1.10	1.2123	10.2
5	1.80	1.7746	1.4	17	0.20	0.2223	11.2
6	1.90	2.0314	6.9	18	1.10	1.1576	5.2
7	0.60	0.5876	2.1	19	4.30	4.5318	5.4
8	0.60	0.6123	2.1	20	0.70	0.7264	3.8
9	0.10	0.1155	15.5	21	0.10	0.1105	10.5
10	1.10	1.1684	6.2	22	1.20	1.1800	1.7
11	2.30	2.4320	5.7	23	0.40	0.4232	5.8
12	0.40	0.4259	6.5	24	2.10	2.1770	3.7
			IV-1				
1	0.10	0.1085	8.5	13	0.40	0.4322	8.0
2	0.90	0.9326	3.6	14	4.00	3.8461	3.8
3	0.20	0.2138	6.9	15	0.80	0.7866	1.7
4	0.30	0.2763	7.9	16	0.10	0.1147	14.7
5	0.70	0.6834	2.4	17	1.80	1.8329	1.8
6	0.20	0.1866	6.7	18	0.40	0.3820	4.5
7	0.40	0.4213	5.3	19	0.30	0.2911	3.0
8	1.90	2.0076	5.7	20	3.30	3.4122	3.4
9	1.20	1.2103	0.9	21	0.20	0.1763	11.9
10	1.10	1.1137	1.2	22	1.10	1.1740	6.7
11	2.10	2.0360	3.0	23	0.10	0.1096	9.6
12	0.10	0.0923	7.7	24	0.40	0.3885	2.9

Table A2. *Cont.*

Sample Number	Measured Value (m)	Predicted Value (m)	Relative Error (%)	Sample Number	Measured Value (m)	Predicted Value (m)	Relative Error (%)
			IV-2				
1	2.00	2.2414	12.1	13	0.20	0.2002	0.1
2	1.30	1.3336	2.6	14	1.50	1.6643	11.0
3	2.90	2.9067	0.2	15	0.30	0.2765	7.8
4	0.10	0.1060	6.0	16	1.80	2.0314	12.9
5	1.30	1.3045	0.3	17	4.10	4.1036	0.1
6	0.20	0.2104	5.2	18	0.00	0.0000	-
7	0.30	0.2861	4.6	19	1.40	1.4326	2.3
8	0.20	0.2310	15.5	20	0.20	0.1913	4.4
9	0.60	0.6210	3.5	21	0.40	0.4140	3.5
10	0.10	0.1098	9.8	22	1.30	1.2631	2.8
11	2.40	2.4464	1.9	23	0.10	0.0861	13.9
12	0.60	0.5811	3.2	24	0.20	0.2029	1.4
			IV-3				
1	1.20	1.2037	0.3	13	0.10	0.1101	10.1
2	0.70	0.7260	3.7	14	0.10	0.0887	11.3
3	0.40	0.3926	1.9	15	1.10	1.1754	6.9
4	0.40	0.3865	3.4	16	0.40	0.4313	7.8
5	0.80	0.7769	2.9	17	0.50	0.5833	16.7
6	1.00	1.0830	8.3	18	0.70	0.6810	2.7
7	0.60	0.5790	3.5	19	1.90	1.7975	5.4
8	0.10	0.0869	13.1	20	1.10	1.0132	7.9
9	0.40	0.4221	5.5	21	2.30	2.3220	1.0
10	0.30	0.3504	16.8	22	0.40	0.4357	8.9
11	0.20	0.1864	6.8	23	0.10	0.0963	3.7
12	0.40	0.4317	7.9	24	2.70	2.6872	0.5
			IV-4				
1	0.60	0.5961	0.7	13	0.40	0.4235	5.9
2	0.30	0.3127	4.2	14	1.20	1.1843	1.3
3	0.90	1.0237	13.7	15	1.20	1.0978	8.5
4	0.40	0.4325	8.1	16	1.70	1.8647	9.7
5	0.20	0.1863	6.9	17	0.20	0.2351	17.6
6	0.40	0.3764	5.9	18	0.40	0.4685	17.1
7	0.10	0.1077	7.7	19	0.20	0.2206	10.3
8	0.10	0.0861	13.9	20	0.70	0.8109	15.8
9	1.80	1.8803	4.5	21	0.20	0.1909	4.6
10	5.20	4.8975	5.8	22	1.60	1.5507	3.1
11	1.20	1.2101	0.8	23	0.50	0.5070	1.4
12	0.10	0.0980	2.0	24	0.50	0.4868	2.6
			IV-5				
1	1.90	2.1133	11.2	13	0.10	0.1133	13.3
2	4.30	4.4106	2.6	14	0.20	0.1941	3.0
3	2.10	2.1055	0.3	15	2.80	3.0476	8.8
4	0.00	0.0000	-	16	1.10	1.2044	9.5
5	1.90	1.7927	5.6	17	1.10	1.1665	6.0
6	0.30	0.3104	3.5	18	1.90	2.0431	7.5
7	0.80	0.7885	1.4	19	0.10	0.0971	2.9
8	1.10	1.1130	1.2	20	1.80	1.7990	0.1
9	0.60	0.5841	2.7	21	4.40	4.1731	5.2
10	0.80	0.7695	3.8	22	0.80	0.9136	14.2
11	0.50	0.4862	2.8	23	0.10	0.1073	7.3
12	0.30	0.3164	5.5	24	1.00	1.0719	7.2

Table A2. *Cont.*

Sample Number	Measured Value (m)	Predicted Value (m)	Relative Error (%)	Sample Number	Measured Value (m)	Predicted Value (m)	Relative Error (%)
			V-1				
1	0.30	0.3174	5.8	13	1.90	2.0348	7.1
2	0.20	0.1867	6.7	14	0.20	0.2160	8.0
3	0.60	0.6673	11.2	15	0.60	0.6231	3.9
4	0.40	0.4176	4.4	16	1.80	1.9677	9.3
5	1.80	1.9135	6.3	17	0.20	0.1995	0.3
6	0.40	0.3652	8.7	18	1.30	1.3549	4.2
7	0.10	0.0837	16.3	19	0.40	0.3956	1.1
8	1.10	1.1966	8.8	20	0.60	0.6394	6.6
9	0.20	0.2135	6.7	21	0.30	0.3166	5.5
10	0.80	0.7869	1.6	22	0.20	0.2237	11.9
11	0.40	0.4345	8.6	23	0.40	0.4130	3.2
12	0.40	0.3799	5.0	24	0.80	0.7668	4.2
			V-2				
1	0.10	0.0868	13.2	13	0.10	0.1012	1.2
2	1.90	2.0754	9.2	14	0.30	0.2741	8.6
3	0.00	0.0036	-	15	0.90	0.8635	4.1
4	0.20	0.2129	6.5	16	0.20	0.1869	6.6
5	0.60	0.5655	5.8	17	1.20	1.3230	10.3
6	0.20	0.2311	15.6	18	1.40	1.4686	4.9
7	0.60	0.5880	2.0	19	0.20	0.2148	7.4
8	1.10	1.0864	1.2	20	1.00	1.0465	4.7
9	0.30	0.3358	11.9	21	4.00	4.3920	9.8
10	0.10	0.1056	5.6	22	1.60	1.6343	2.1
11	0.50	0.4686	6.3	23	0.40	0.3864	3.4
12	4.30	4.9357	14.8	24	2.10	2.0861	0.7
			V-3				
1	0.00	0.0000	-	13	0.40	0.4317	7.9
2	0.10	0.0969	3.1	14	1.30	1.2765	1.8
3	0.20	0.1864	6.8	15	1.20	1.2210	1.8
4	2.40	2.3556	1.9	16	0.10	0.1125	12.5
5	0.70	0.7436	6.2	17	5.20	4.9361	5.1
6	0.10	0.0941	5.9	18	1.70	1.7654	3.8
7	0.40	0.4430	10.8	19	0.40	0.3575	10.6
8	0.10	0.0865	13.5	20	0.70	0.6690	4.4
9	0.10	0.1106	10.6	21	0.20	0.2147	7.4
10	0.80	0.7842	2.0	22	1.80	1.9345	7.5
11	0.10	0.1045	4.5	23	0.20	0.2144	7.2
12	0.10	0.0879	12.1	24	4.10	3.8160	6.9
			V-4				
1	2.80	2.9726	6.2	13	1.10	1.1249	2.3
2	3.30	2.7489	16.7	14	1.10	1.1592	5.4
3	0.30	0.2537	15.4	15	1.10	1.1498	4.5
4	2.30	2.4276	5.5	16	0.10	0.0840	16.0
5	0.50	0.4861	2.8	17	1.10	1.2486	13.5
6	2.10	2.0452	2.6	18	2.90	3.0465	5.1
7	0.10	0.0984	1.6	19	0.70	0.7238	3.4
8	1.90	2.0675	8.8	20	0.50	0.4731	5.4
9	0.30	0.3529	17.6	21	0.10	0.0823	17.7
10	1.90	1.8643	1.9	22	0.10	0.1039	3.9
11	1.10	1.2342	12.2	23	1.20	1.2728	6.1
12	0.10	0.0930	7.0	24	0.20	0.1637	18.2

Table A2. *Cont.*

Sample Number	Measured Value (m)	Predicted Value (m)	Relative Error (%)	Sample Number	Measured Value (m)	Predicted Value (m)	Relative Error (%)
				V-5			
1	0.80	0.8637	8.0	13	0.10	0.0900	10.0
2	2.70	2.8150	4.3	14	2.00	2.2093	10.5
3	1.90	1.8938	0.3	15	0.50	0.5076	1.5
4	0.80	0.6812	14.9	16	4.40	4.6037	4.6
5	0.40	0.4193	4.8	17	1.30	1.2138	6.6
6	0.30	0.2941	2.0	18	0.30	0.3204	6.8
7	0.20	0.1738	13.1	19	1.20	1.1760	2.0
8	0.40	0.4229	5.7	20	1.80	1.7681	1.8
9	0.40	0.3843	3.9	21	1.00	1.0375	3.8
10	0.40	0.3715	7.1	22	0.40	0.4638	16.0
11	1.20	1.1534	3.9	23	1.50	1.6032	6.9
12	0.90	0.8633	4.1	24	0.70	0.6821	2.6

References

1. Cai, M.F.; Xue, D.L.; Ren, F.H. Current status and development strategy of metal mines. *Chin. J. Eng.* **2019**, *41*, 417–426. (In Chinese)
2. Li, C.N.; Ren, F.Y.; Xu, X.H. Analysis of loss and dilution in mineral resources exploitation in Chinese. *J. Nat. Resour.* **2000**, *1*, 36–39. (In Chinese)
3. Pakalnis, R.C.T.; Poulin, R.; Hadjigeorgiou, J. Quantifying the cost of dilution in underground mines. *Int. J. Rock Mech. Min. Sci. Geomech. Abstr.* **1995**, *47*, 1136–1141.
4. Parker, H.M. Reconciliation principles for the mining industry. *Min. Technol.* **2012**, *121*, 160–176. [CrossRef]
5. Crawford, G.D. Dilution and Ore Recovery. *Pincock Perspect.* **2004**, *60*, 1–4.
6. Ebrahimi, A. An attempt to standardize the estimation of dilution factor for open pit mining project. In Proceedings of the World Mining Congress, Montreal, QC, Canada, 11–15 August 2013.
7. Clark, L. Minimizing Dilution in Open Stope Mining with Focus on Stope Design and Narrow Vein Longhole Blasting. Ph.D. Thesis, University of British Columbia, Vancouver, BC, Canada, 1998.
8. Liu, X.G.; Zhang, G.L.; Liu, X.B. Analysis of ore loss and dilution in pillarless sublevel caving. *Met. Mine* **2006**, *1*, 53–60. (In Chinese)
9. Luo, Z.Q.; Zhang, B.; Liu, X.M. Calculation method for mining loss and ore dilution based on CMS precision survey. *Met. Mine* **2007**, *10*, 84–88. (In Chinese)
10. Tait, L. An Investigation into Using Artificial Neural Networks for Empirical Design in the Mining Industry. Ph.D. Thesis, University of British Columbia, Vancouver, BC, Canada, 1998.
11. Wang, J. Influence of Stress, Undercutting, Blasting and Time on Open Stope Stability and Dilution. Ph.D. Thesis, University of Saskatchewan, Saskatoon, SK, Canada, 2004.
12. Papaioanou, A.; Suorineni, F.T. Development of a generalised dilution-based stability graph for open stope design. *Min. Technol.* **2016**, *125*, 121–128. [CrossRef]
13. Stewart, P.C.; Trueman, R. Strategies for minimising and predicting dilution in narrow-vein mines—NVD Method. In Proceedings of the Narrow Vein Mining Conference, Ballarat, Australia, 14–15 October 2008.
14. Jang, H.; Topal, E.; Kawamura, Y. Decision support system of unplanned dilution and ore-loss in underground stoping operations using a neuro-fuzzy system. *Appl. Soft Comput.* **2015**, *32*, 1–12. [CrossRef]
15. Jang, H.; Topal, E.; Kawamura, Y. Illumination of parameter contributions on uneven break phenomenon in underground stoping mines. *Int. J. Min. Sci. Technol.* **2016**, *26*, 1095–1100. [CrossRef]
16. Brady, T.; Martin, L.; Pakalnis, R. Empirical approaches for opening design in weak rock masses. *Min. Technol.* **2005**, *114*, 13–20. [CrossRef]
17. Wang, J.; Milne, D.; Pakalnis, R. Application of a neural network in the empirical design of underground excavation spans. *Min. Technol.* **2002**, *111*, 73–81. (In Chinese) [CrossRef]
18. Pakalnis, R.; Eng, P.; Brady, T. Weak rock mass design for underground mining operations. In Proceedings of the International Workshop on Rock Mass Classification in Underground Mining, Vancouver, BC, Canada, 31 May 2007.

19. Zhao, X.D.; Xu, S. *Principle and Application of 3D Laser Digital Surveying Technology in Mine Engineering*; Metallurgical Industry Press: Beijing, China, 2016; pp. 99–163.
20. Wu, W.; Wang, J.; Cheng, M.; Li, Z. Convergence analysis of online gradient method for BP neural networks. *Neural Netw.* **2011**, *24*, 91–98. [CrossRef] [PubMed]
21. Yi, J.; Wang, Q.; Zhao, D.; Wen, J. BP neural network prediction-based variable-period sampling approach for networked control systems. *Appl. Math. Comput.* **2007**, *185*, 976–988. [CrossRef]
22. Zhao, J.; Wang, F. Parameter identification by neural network for intelligent deep drawing of axisymmetric workpieces. *J. Mater. Process. Technol.* **2005**, *166*, 387–391. [CrossRef]
23. Wang, W.; Yao, Y.; Ma, Z. Model of Compressor Performance Prediction Based on Error Back-propagation Artificial Neural Network. *Fluid Mach.* **2005**, *33*, 21–24. (In Chinese)
24. Gorman, P.R.; Sejnowski, T.J. Analysis of hidden units in a layered network trained to classify sonar targets. *Neural Netw.* **1988**, *88*, 75–89. [CrossRef]
25. Wang, Q.; Meng, W.; Ma, Y.; Hu, X. Prediction of Chlorophyll-a Concentration in Dahuofang Reservoir Based on BP Neural Network. *J. Northeast. Univ. Nat. Sci.* **2013**, *34*, 1792–1795. (In Chinese)
26. Zhao, X.D.; Niu, J.A. Stability Evaluation and Parameter Optimization of Stope Based on Extended Mathews Stability Graph Method. *Met. Mine* **2020**, in press.